eGaN FETs for Lidar – Getting the Most Out of the EPC9126 Laser Driver

EPC
EFFICIENT POWER CONVERSION

John S. Glaser, Director of Applications Engineering; Efficient Power Conversion Corporation

Lidar is a form of radar where the electromagnetic radiation happens to be in the optical band [1, 2]. In the last few years, one particular form of lidar, time-of-flight (TOF) distance measurement, has become popular. If a laser is used as the optical source, one can measure the distance of a small spot even at a long range. When combined with steerable optics, one can sweep the spot distance measurement and map objects in 3-D space.

EPC has developed the EPC9126 and EPC9126HC laser drivers to demonstrate the performance of eGaN FETs in lidar systems, and to advance the lidar state of the art [3, 4]. The EPC9126 and EPC9126HC are both provided with Quick Start Guides (QSG) that provide basic information on getting up and running along with schematics and bills of materials. Layout files for the drivers are also freely available.

However, while the basic principle of the laser drivers seems simple, the high speeds, voltages, and currents result in the dominance of parasitic components that many engineers are used to ignoring or designing away. This document was written to answer common questions and to provide more depth on laser driver design, so that the user can get the most out of their driver.

Please note that this application note is intended as a complement to the QSG, and the user should have both handy when learning about and applying the EPC9126 and EPC9126HC.
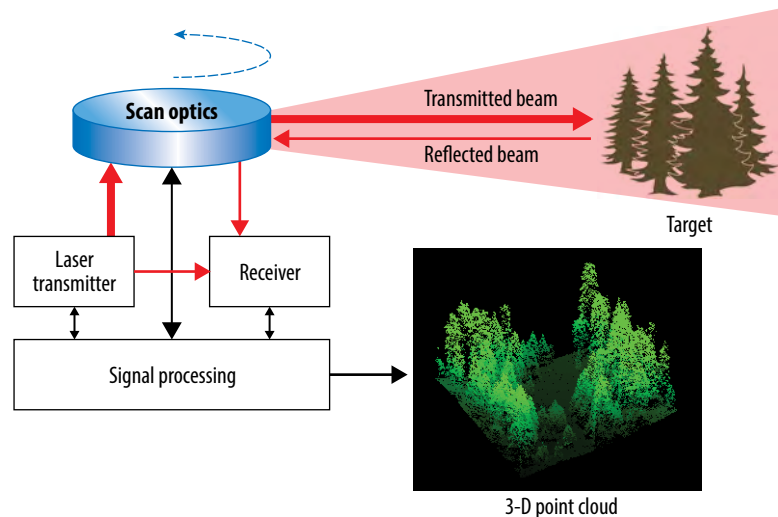

Figure 1. Basic lidar system

Lasers and pulse requirements

TOF lidar usually uses near-infrared (NIR) semiconductor laser diodes, either side-emitting epitaxial lasers or vertical cavity surface emitting lasers (VCSELs). Some typical laser diodes are shown in Figure 2 [5, 6]. Electrically, the laser diode behaves as a rectifier. When forward biased above a certain threshold current, it emits laser radiation with the output optical power approximately proportional to the forward current. Thus, if we drive it with a pulse of current, we get a pulse of laser light [7]. The laser optical pulse has two main parameters: pulse width and energy. These two factors have a large effect on the distance resolution and the range, respectively.
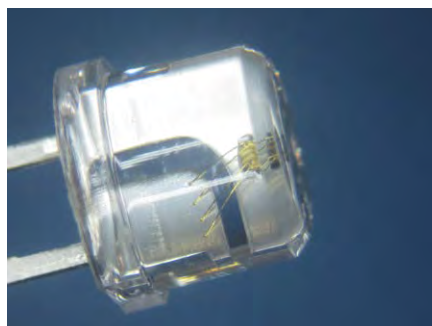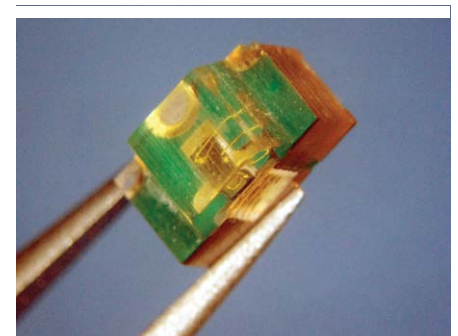
SPL PL90_3   **TPGAD1S09H**

Figure 2. Some typical laser diodes used for TOF lidar.

The pulse width of the transmitted optical signal has a great influence on the distance resolution of a lidar system [8, 9]. Figure 3 helps show why this is the case. If we look at the top case, we send narrow pulses of light out from the lidar. Since the light pulse must travel to the target, be reflected, and travel back, for a target at distance d, the time t_d between pulse transmission and reception is:

$$t_d = 2d/c \qquad (1)$$

Where c is the speed of light in air, approximately 30 cm/ns (about 1 foot/ns for the imperialists among us). By measuring the time t_d, we can compute the distance. Now suppose that we send longer duration pulses, as shown in the bottom case. We see that if the pulse length becomes long enough, the reflected pulses begin to overlap, and it becomes harder to distinguish features in the environment.

For an idea of what pulse lengths are desirable in practice, consider an electrical current pulse width of 1 ns driving the laser diode, which corresponds to an optical pulse length of 30 cm. As features of the target approach 15 cm, the received pulses begin to overlap and become harder to distinguish. While various signal processing techniques can improve the resolution for a given pulse width, it is clear that a shorter pulse gives better inherent precision, and that pulses on the order of a few nanoseconds or less are desirable for human-scale resolution.

Pulse energy determines the range of the lidar. As demand for better resolution drives designs towards narrower pulses, the diode current must increase in order to maintain sufficient pulse energy. Typical pulse current can range from a few amps to hundreds of amps. A number of laser diodes are specified

with nominal pulse currents in the range of several tens of amps. Under typical data sheet test conditions, e.g. Pulse repetition frequency (PRF) = 1 kHz, pulse width t_w = 100 ns, peak current I_{DLpk} = 30 A, operating temp T_{OP} = 23-25℃, the peak electrical input power can approach 300 W for a triple junction edge emitting laser. The average test duty cycle is often ≤ 0.1% to prevent overheating of the laser die. It is possible to operate these laser diodes at higher currents with shorter pulse widths and obtain greater peak optical power.

In summary, typical laser diode requirements for commercial off-the-shelf laser diodes in lidar systems suitable result in desired peak pulse current ranges from a few amps to a few hundred amps, with pulse widths from 1 ns to 10 ns. In the next section, we will see how to obtain these extreme pulses.
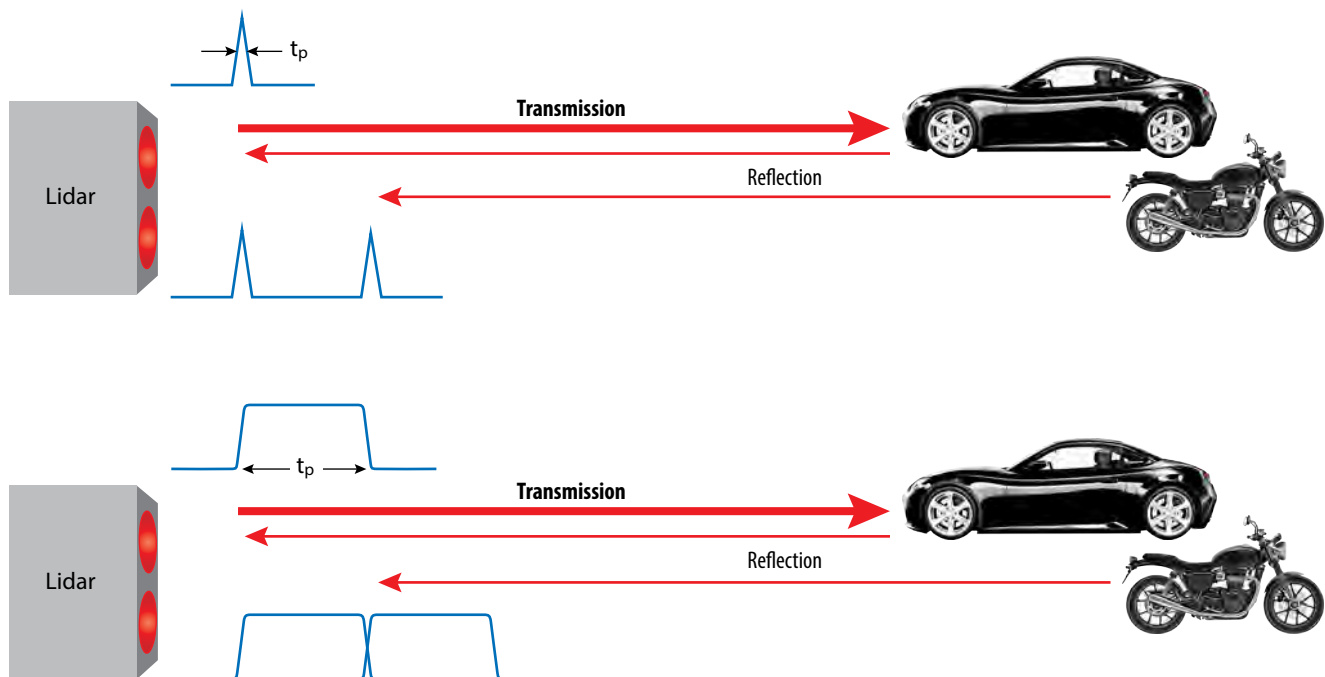

Figure 3. Effect of lidar pulse width on resolution. Top: narrow pulses allows reflections to be easily distinguished. Bottom: wider pulses can overlap, making them harder to distinguish and reducing distance resolution.

Laser drivers

A typical pulsed laser driver for lidar uses a semiconductor switch in series with the laser and an electrical energy source. Performance is limited by stray inductance and the speed of the semiconductor power switch. Within the last decade, cost-effective gallium nitride (GaN) power FETs have become commercially available, with significantly lower inductance and switching figures of merit (FOMs) up to 10x better than comparable silicon MOSFETs [10]. Figure 4 shows the EPC2016C FET, a 100 V eGaN FET capable of 75 A pulses [11].

The greatly improved performance of eGaN FETs versus the older silicon MOSFET technology translates to much faster switching for a given peak current capability, enabling currents >100 A and pulse widths <2 ns with a laser load [13, 14], although these cannot be met simultaneously (yet!).

There are many kinds of laser driver topologies, but for high power there are two primary candidates: the leading edge controlled resonant laser driver and the current limited dual edge controlled driver. Since the resonant laser driver is the most common for high speed applications, most of the discussion will be around this type of driver.

EPC9126 and EPC9126HC laser diode drivers

The EPC9126 laser driver is a versatile platform on which to test the performance of eGaN FETs and laser diodes. The PCB for the EPC9126 and EPC9126HC is identical. The two drivers have a few component differences, with the result being that the off-the-shelf EPC9126 will have a lower peak current and a shorter pulse, whereas the EPC9126HC will have a higher output current with a longer duration pulse. The key differences are summarized in Table 1. Aside

from these differences, the boards are identical and unless otherwise specified, everything in this note applies to both boards, which will be collectively referred to as the EPC9126xx.

As shipped, these are both configured as resonant laser drivers. The basic operation of these drivers along with the corresponding design equations are discussed in the following section.

Resonant capacitive discharge laser driver design

Figure 5 shows a simplified schematic of a resonant capacitive discharge laser driver, and Figure 6 shows the main waveforms.
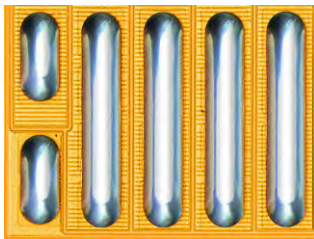

Figure 4. EPC2016C 100 V, 75 A, 16 mΩ eGaN FET measures 2.1 mm x 1.6 mm. The EPC2212 is an automotive qualified (AEC-Q101) part with same footprint and similar ratings [12].

Component	EPC9126	EPC9126HC
FET	EPC2016C / EPC2212	EPC2001C
FET pulse current rating	75 A	150 A
Current shunt	102 mΩ	94 mΩ
Resonant capacitance	1.1 nF	2.8 nF

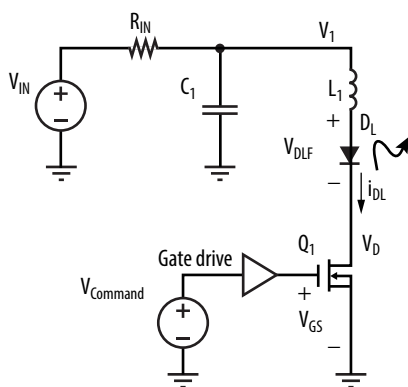Table 1. Differences between EPC9126 and EPC9126HC

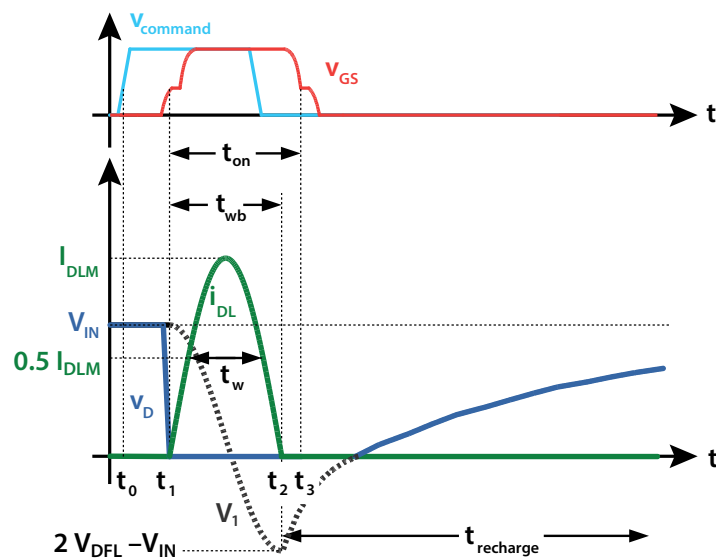Figure 5. Capacitive discharge resonant driver

Figure 6. Key waveforms for capacitive discharge resonant driver of Figure 5.

Assuming that Q_1 is an ideal switch and D_L an ideal diode with a fixed forward voltage drop V_{DLF}, The driver works as follows: Q_1 starts in the off-state, so $i_{DL} = 0$. The capacitor voltage $v_1 = V_{IN}$, having been charged through R_1. At $t = t_0$, $v_{command}$ triggers the gate drive, turning Q_1 fully on at $t = t_1$ and discharges C_1 through the laser D_L and inductor L_1. C_1 and L_1 form a resonant network, hence i_{DL} and v_{C1} ring sinusoidally. The effective initial capacitor voltage is $V_{C1,0} = V_{IN} - V_{DLF}$ due to the laser diode forward drop. At $t = t_2$, i_{DL} returns to zero and $v_{C1} = 2 V_{DLF} - V_{IN}$. At this point D_L prevents the current from reversing and C_1 recharges via R_1. Switch Q_1 is turned off before V_1 crosses zero at $t = t_3$.

The capacitor charging time constant τ_{chrg} and the resonant period t_{res} are

$$\tau_{chrg} = R_1 C_1 \tag{2}$$

$$t_{res} = 2\pi\sqrt{(L_1 C_1)} = 2t_{wb} \tag{3}$$

Typically, $\tau_{chrg} \gg t_{res}$, so R_1 has little effect on the L_1–C_1 resonance. The resonant characteristic impedance R_0 and the full width half maximum (FWHM) pulse width t_w are

$$R_0 = \sqrt{\frac{L_1}{C_1}} \tag{4}$$

$$t_w = t_{res}\frac{\pi - 2sin^{-1}\frac{1}{2}}{2\pi} = \frac{t_{res}}{3} \tag{5}$$

This laser driver topology has the following benefits

- The topology utilizes stray inductance.
- Stable pulse shape
- Pulse energy is set via the value of V_{IN}
- The switch is ground-referenced for simple drive
- Only gate turn-on needs precise control (single edge control)
- Laser current pulse width can be shorter than gate drive minimum pulse width

Effect of stray inductance

We can calculate the peak laser diode current I_{DLpk} using the following equation:

$$I_{DLpk} = \frac{V_{IN} - V_{DLF}}{R_0} \tag{6}$$

The inductance has a large effect on the design. From (3), (4), (5), and (6), we solve for V_{IN} to find

$$V_{IN} = \frac{2\pi L_1}{3t_w}I_{DLpk} + V_{DLF} \tag{7}$$

Figure 7 shows the calculated voltage V_{IN} from (7) versus L_1 for a 30 A, 4 ns pulse with a 9 V forward diode drop on the laser. It is clearly seen that the required V_{IN} increases linearly with L_1 for a given laser and pulse shape.

Driver switch properties

The analysis above assumes an ideal switch, but practical semiconductor switches have non-zero switching times and saturation current limits. In addition, switches and their packages can have significant inductance which not only increases the required voltage for a given pulse shape, but also slows switch turn-on.

In the past, the switch technology of choice was a silicon power MOSFET. However, as lidar system designers strive to get more performance, silicon power MOSFETs have become the major limiting factor for two reasons. The first is the large gate charge due

to the large die size needed to meet the current and voltage requirements. This greatly slows the turn-on of the MOSFET [15]. Second, large MOSFETs are vertical devices with connections on both sides of the die. This forces the use of an external package, which adds substantial inductance in both the power loop and the gate drive loop [16]. The former results in a higher voltage requirement and an even larger die, and the latter further slows the device turn on.

In the last several years, new power FETs based on GaN have become commercially available. GaN FETs have several overwhelming advantages for lidar applications compared to silicon MOSFETS. First, they have up to 10x lower input capacitance C_{ISS} than MOSFETs of comparable current rating [17], enabling the GaN FET to turn on much faster. Second, GaN FETs are a lateral device, which allows the use of a wafer level chip scale package (WLCSP). The WLCSP provides extremely low inductance, excellent thermal performance, high reliability, and minimal added cost. Finally, GaN FET die are much smaller than silicon power MOSFETs of comparable voltage and current rating, further reducing inductance, and allowing tight spacing of adjacent lasers for applications such as multi-channel lidar [18].
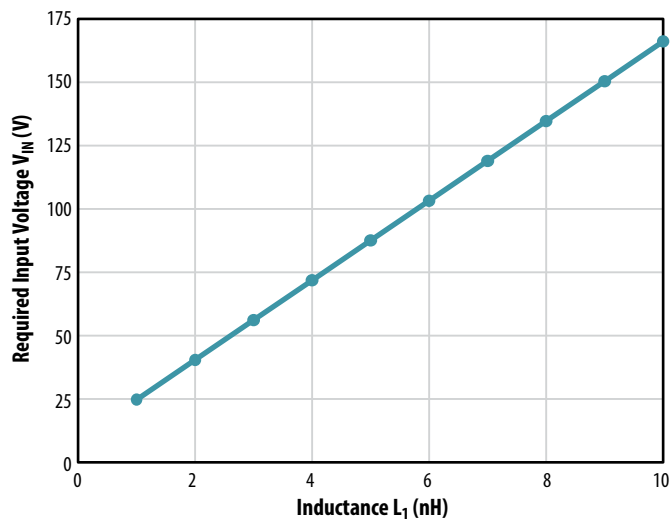

Figure 7. Bus voltage V_{IN} versus inductance L_1 for $I_{DLpk} = 30 A$, $t_w = 4 ns$, and $V_{DLF} = 9 V$.

Basic design process

Now we can put the above information together in order to do the design of a resonant lidar driver. We start with some specifications on the laser pulse, which will generally result from the system design. These requirements are:

- Pulse peak amplitude I_{DLpk}

- Full width half maximum (FWHM) pulse width t_w

- Pulse repetition frequency PRF

- Laser diode voltage drop V_{DLF}

Once the basic pulse requirements have been chosen, the next factor needed to complete the design is the power loop inductance L_1. The determination of L_1 is discussed in Section 3.4, but for now, assume we have a good estimated value.

To determine the value of resonant capacitor C1, we use (4) and (6) to get

$$C_1 = L_1 \left(\frac{I_{DLpk}}{V_{IN} - V_{DLF}} \right)^2 \qquad (8)$$

The value of recharge resistor R_1 is determined from (2), so that

$$R_1 = \frac{\tau_{chrg}}{C_1} \qquad (9)$$

Since $\tau_{chrg} \gg t_{res}$, we simply need to pick a large enough value of τ_{chrg}. Because of thermal limitations forcing the pulse duty cycle to be typically less than 1% or so, the value of R_1 does not usually need precise determination. This is discussed further in Section 6.4 for those needing to operate at higher duty cycle values.

Finally, the required bus voltage V_{IN} is determined from (7), which together with I_{DLpk} is used to select the appropriate part number for FET Q_1. Together, (7), (8) and (9) determine the remaining values to complete the design.

Determination of power loop inductance

We have already seen that the required input voltage increases nearly linearly with the laser inductance, and input voltage determines the rating of the FET and the capacitors. Furthermore, the laser driver bus voltage has to come from somewhere, most likely another boost converter in the circuit. The more that L_1 is reduced, the simpler and lower cost the rest of the design will be. The core principles of minimizing PCB inductance are explained in depth in [19], which covers a variety of useful techniques for reducing layout inductance. The article shows that with the eGaN FET's chip-scale package, the power loop inductance contribution of the FET, PCB, bus capacitance, and current sensing shunt (if desired) can be kept well below 1 nH, and can approach values below 500 pH. The stray inductance of the EPC9126xx is on the order of 1 nH, depending on the FET and the mounting position of the load. The value is higher than the best achievable value since this was a tradeoff taken to increase the versatility of the design, especially the ability to accommodate different laser packages.

Now, we turn to other sources of inductance, and the main one is the laser. As seen earlier, a through-hole laser can be expected to contribute about 5 nH in the best case, and often much higher. A surface mount laser will contribute something closer to 1 to 3 nH, which makes the laser the dominant inductance. Note that most of the laser inductance comes from the laser package, including wire bonds. Laser manufacturers have become aware that the laser package inductance can dominate performance, so one should expect progress in this area in the near future.

Unfortunately, the value for L_1 is difficult to know exactly at the beginning of the design. This means that it is likely that some iteration will be necessary. For an initial design, consider giving yourself some additional voltage margin on the FET, which will allow one to overcome a certain amount of unanticipated inductance.

EPC9126xx Hardware Driver Design

A typical connection diagram for the EPC9126xx laser driver is shown in Figure 8. A complete description of connection and operation is given in the Quick Start Guides [20, 21], but is it useful to review the diagram here.

All signal I/O uses SMA connectors. The design includes voltage test points comprising embedded transmission line probes with the output taken at J3, J7, J9, and J10. The output of a current measurement shunt is available from J6. Details of the design can be found in [3, 4], including Gerber layout files and a full schematic. The layout was designed to minimize the total inductance in keeping with the principles in [19].

A photograph of the driver, along with an expanded view of the key section of the design is shown in Figure 8. To minimize inductance L_1, both the energy storage capacitor C_1 (C_{11}, C_{12}, C_{13}, C_{14}, C_{15} on the PCB) and the current measurement shunt (R_{12}, R_{13}, R_{14}, R_{15}, R_{16}) are comprised of five 0402 size surface mount packages connected in parallel. The spacing between the top plan and the ground plane is 250 μm (10 mil) minimize inductance. To minimize cost, no blind, buried, or microvias are used.
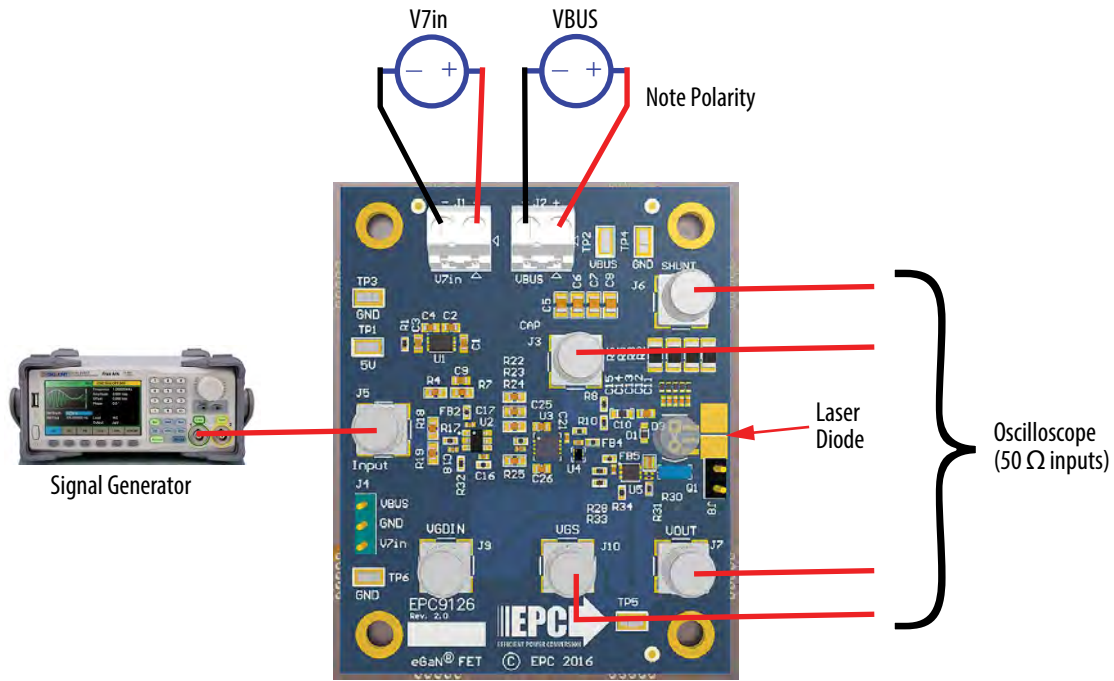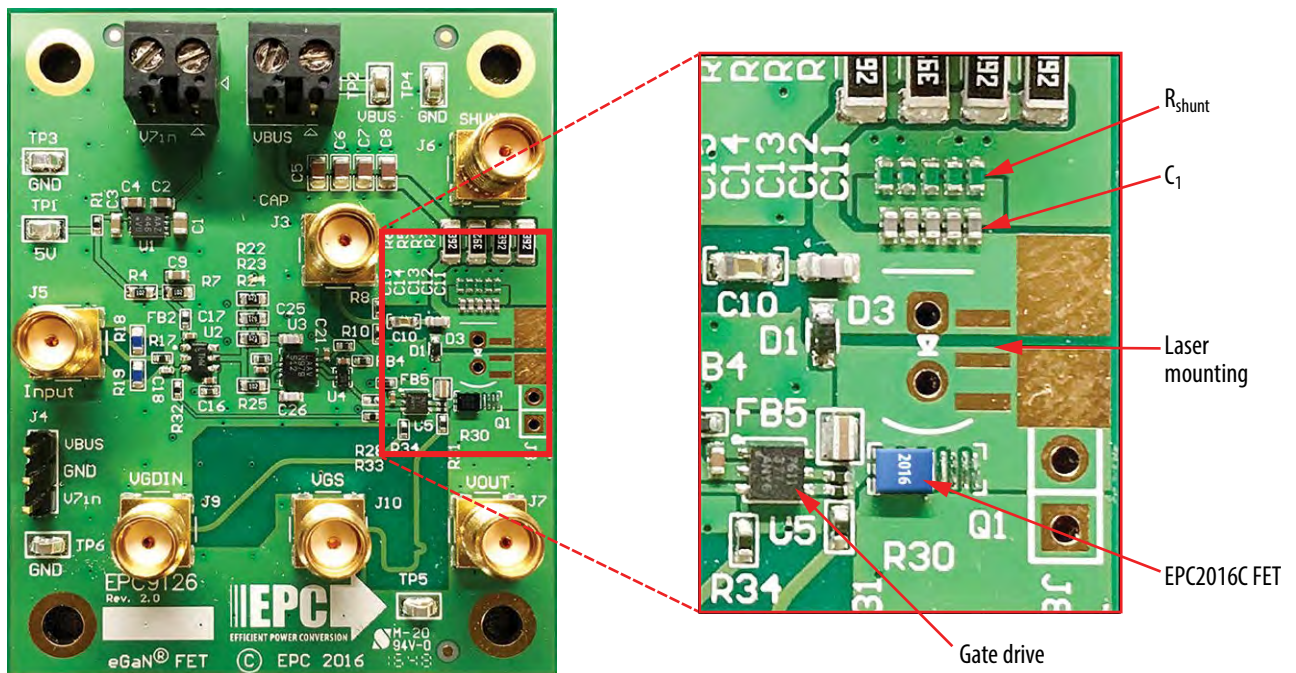

Figure 8.

Figure 9. EPC9126 laser driver with GaN FET for experimental validation.

To get good shunt performance for current measurement, it was necessary to mount the shunt resistors upside down, which yielded a reduction in shunt equivalent series inductance from 200 pH to 40 pH, and a corresponding fourfold increase in shunt bandwidth [13]. This is discussed further in the section Current Sensing (page 9).

Experimental Results

The EPC9126 and EPC9126HC have both been tested with the Excelitas TPGAD1S09H surface mount laser, which at the time of writing is the lowest inductance surface mount high power pulse laser that is readily available. In each case, the circuit test results are given with an input voltage of 75 V.

EPC9126

The power loop inductance L_1 is estimated to be 2.3 nH. If we design for $I_{DLpk} = 35$ A and a 3.5 ns pulse width, this gives a $C_1 = 1.2$ nF and $V_{IN} = 60$ V. The capacitor value used was $C_1 = 1.1$ nF since this was the closest that could be achieved with standard component values. NP0/C0G ceramic capacitors were used due to their stable capacitance and low loss. Test results for $V_{IN} = 75$ V are shown in Figure 10. A peak current, $I_{DLpk} = 35$ A, is reached with $t_w = 3.4$ ns. This amounts to a peak electrical power input to the laser $P_{DLpk} > 300$ W. The discrepancy in the results and calculations results from the different capacitance value, inductance estimation error, extra voltage drop on the shunt, and the fact that the laser diode voltage drop is not really a fixed value.

EPC9126HC

The power loop inductance L_1 is estimated to be 2.0 nH, with the reduction due to the wider footprint of the EPC2001C compared to the EPC2016C. If we design for $I_{DLpk} = 70$ A and a 5 ns pulse width, this gives a $C_1 = 2.85$ nF and $V_{IN} = 78$ V. The capacitor value used was $C_1 = 2.8$ nF since this was the closest that could be achieved with standard component values. NP0/C0G ceramic capacitors were used due to their stable capacitance and low loss. Test results for $V_{IN} = 75$ V are shown in Figure 10. A peak current, $I_{DLpk} = 63$ A, is reached with $t_w = 5.0$ ns. This amounts to a peak electrical power input to the laser $P_{DLpk} > 1300$ W. The discrepancy in the results and calculations results from the slightly different capacitance value, inductance estimation error, extra voltage drop on the shunt, and the fact that the laser diode voltage drop is not really a fixed value.

Tips and tricks for the 9126

The EPC9126xx has a great deal of flexibility and can be used as a base from which to try out new ideas or gain deeper understanding of real component behavior for fast, high current pulses. This section provides some further detail on the design along with suggestions on different directions to pursue further. Figure 12 is a block diagram of the EPC9126x and provides a useful reference for this sections.
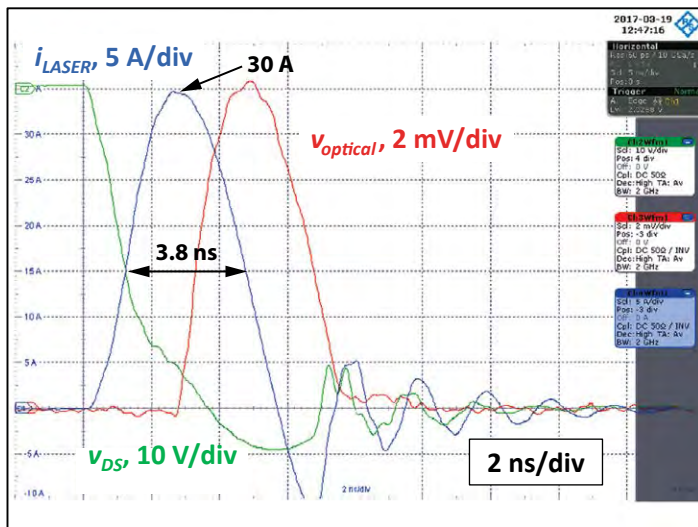

Figure 10. Experimental results for EPC9126 laser driver fitted with an EPC2016C GaN FET with $V_{IN} = 75$ V. A peak current $I_{DLpk} = 35$ A is reached with $t_w = 3.4$ ns.
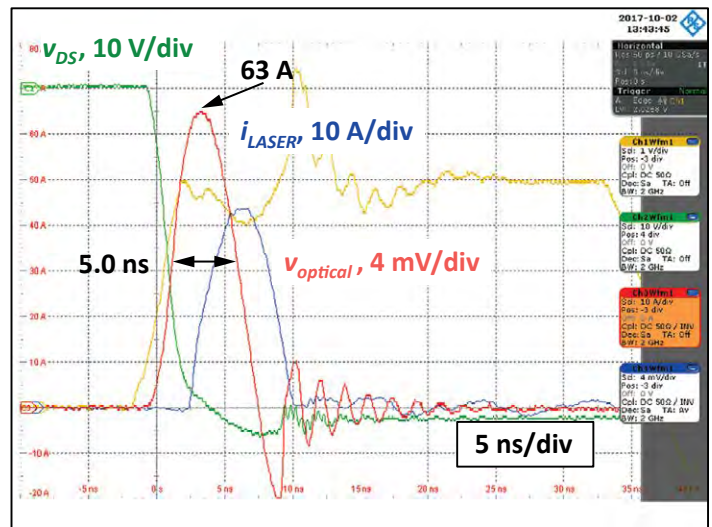

Figure 11. Experimental results for EPC9126HC laser driver fitted with an EPC2001C GaN FET with $V_{IN} = 75$ V. A peak current $I_{DLpk} = 63$ A is reached with $t_w = 5.0$ ns.
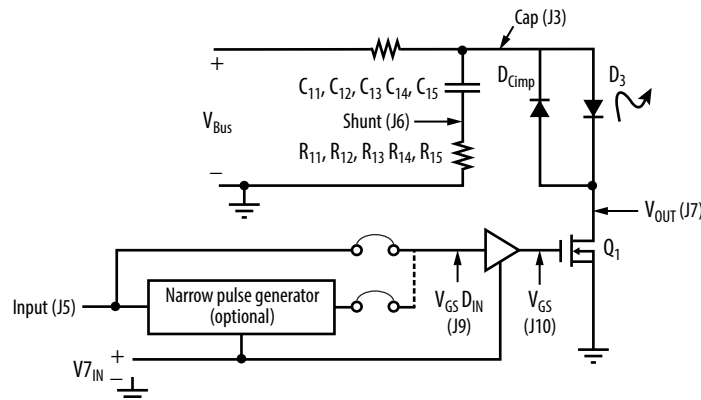

Figure 12. Block diagram of the EPC9126xx.

Inputs and outputs

The high speeds involved in laser pulse drivers dictate the use of RF techniques, in particular the use of controlled impedances and the use of a 50 Ω standard impedance for cables and measurements. If you are not sure what this means, there are some good references to get started, as a full explanation is beyond the scope of this article. A good reference for those new to the topic is [22].

The input is terminated with a low inductance 50 Ω resistance (two 100 Ω resistors in parallel), and feeds directly into a comparator with a 2.5 V threshold. When connected to a pulse generator with a 50 Ω cable, there will be a minimum of ringing and reflection. If it is desired to drive the board with a logic gate directly, please keep in mind that the output impedance of many logic gates can be a few hundred ohms, meaning that they will not drive the input to high enough voltage. In this case, the input terminating resistors can be removed, but the connection to the logic gate must be made in a manner to minimize any ringing or pulse reflections. If this sounds unfamiliar, please review the reference above.

All the outputs are designed to operate properly into a 50 Ω load. This is best accomplished with the use of a 50 Ω cable connecting to an oscilloscope with a 50 Ω internal input. Please note that the use of external 50 Ω terminations at the scope input, with a scope input set to 1 MΩ, will work, but will be bandwidth limited by the typical input capacitance of the 1 MΩ input connection. This capacitance will often limit the measurement bandwidth to < 200 MHz, giving a minimum measurement rise time on the order of 1 ns, which make things look a lot slower than they actually are.

Laser mounting

The EPC9126xx was designed for flexibility in the package and mounting of the laser or other load. It has 100 mil spaced through holes for mounting of leaded laser diode packages. In addition, it has a footprint for an Excelitas surface mount laser diode. Finally, it has bare pads that allow flexible mounting of different packages, or even bare laser die. Figure 13 shows some of the possible ways of mounting lasers.

Resonant capacitors

Once the inductance has been minimized, the main parameters under the designer's control are voltage and resonant capacitance. Resonant capacitors should be NPO/C0G ceramic dielectric or some other cap with low loss and linear, stable dielectric, such as porcelain, glass, or mica.
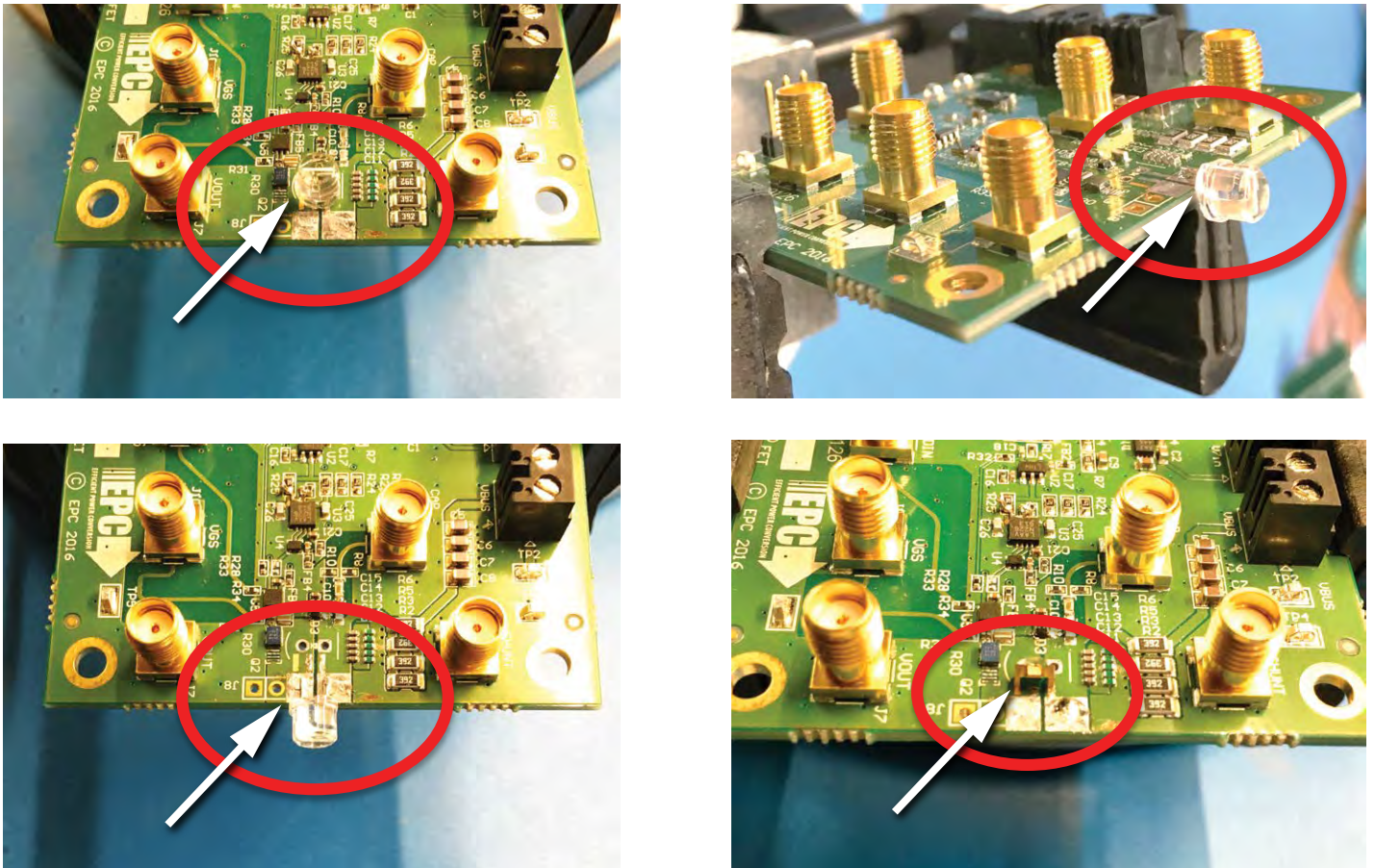

Figure 13. Different ways of mounting lasers or other loads to the EPC9126xx. Upper left: conventional through-hole mounting. Upper right: laser anode lead on top and cathode lead on bottom of PCB. Lower left: both leads of laser on top side. Lower right: surface mount laser.

Charging resistors

The resonant capacitor is charged through the charging resistor R_1 (formed by the parallel combination of R_2, R_3, R_5, R_6 on the EPC9126xx), with a time constant τ_{chrg} given by (1). Since it takes $t = 5\tau_{chrg}$ to charge the resonant cap to > 99% of the final value, we can set the max pulse repetition frequency to PRF = 1/5 · τ_{chrg}. If a designer wants a higher value of PRF, they can either accept some droop in the laser output, or they can reduce the value of R_1. Reducing R_1 will allow additional current to flow in Q_1 when on, but this is likely to be acceptable for $5\tau_{chrg} \gg t_w$.

For an ideal resonant system like that shown in Figure 5 and the associated waveforms in Figure 6, we can see that except for the very first time the capacitor C_1 is charged, the initial state of the capacitor is $V_{C1}(t2) = V_{IN} - 2V_{DFL}$. It is a good approximation that during recharge, all power dissipation occurs in R_1, and the energy dissipated in R_1 will be

$$E_{R1chrg} = 2C_1(V_{BUS} - V_{DFL})^2 \qquad (10)$$

Note that this is independent of R_1. The power dissipation will be

$$P_{R1chrg} = PRF \cdot E_{R1chrg} \qquad (11)$$

At high PRF, this power dissipation can be substantial and is in addition to the power dissipation in the laser itself. If the power dissipation is too large, different recharge methods such as boost converters should be considered. These are beyond the scope of this article.

Transmission line probes

All sense measurement SMAs, except for the shunt measurement, use the transmission line voltage probe principle to obtain waveform fidelity at sub-ns time scales. Such probe typically have a relatively low probing impedance, on the order of 500 to 5k, but the impedance is nearly purely resistive and the bandwidth can be very high, i.e. multiple GHz. These probes are built into the PCB to allow near ideal connection to the node of interest, thus improving waveform fidelity and repeatability. They also won't slip off the measurement points, which is an important consideration when measuring the high voltages in the circuit! The basic principles of such probes are discussed in [23].

In order to get useful measurements with the built-in probes, one has to take into account the following three properties. First, they must be connected to an oscilloscope with the scope input set to 50 Ω. The use of a 1 MΩ input with a 50 Ω terminator will severely limit the bandwidth for almost all scopes and is not recommended. Second, each built-in probe has its own attenuation factor that must be considered. Third, the low impedance of the probe means that for points with a large average DC voltage, e.g. drain voltage, substantial power dissipation can occur. To prevent this dissipation, the test points for high voltage measurements include a DC blocking capacitor. This forms a high pass filter that has little effect for typical waveforms of interest. However, if long pulse widths are used, these test points may yield erroneous results, and an external probe should be used. The built-in transmission line probes have been verified to produce near-identical results to a Tektronix P9158 3 GHz transmission line probe [24], so their estimated bandwidth is at least 3 GHz.

Current sensing

Ahh, current sensing… the bane of power electronics!

There are both pros and cons to current sensing in pulse laser drivers. The pros include verification of operation, timing determination of the laser pulse, control of optical power for maximizing range while remaining eye safety. However, current sensing has a long list of cons, including added inductance, increased power dissipation, poor waveform accuracy, cost, and reduced laser drive voltage to overcome inductance.

Current measurement capability is included in the EPC9126xx in the form of a resistive current shunt formed from five 0402 resistors to minimize added power loop inductance. The low duty cycle of laser drivers allows the use of such small resistors even at very high currents. In order to include affordable current sensing while still minimizing the negative

impact on performance, some compromises on the current shunt were made. These compromises can result in considerable distortion of the current waveform.

Normally, it is desired to have a very small resistance value for the shunt to minimize voltage drop due to the high peak current. Unfortunately, even the very small inductance of five parallel 0402 size resistors can have a large effect on shunt impedance and hence the measurement itself. A conservative estimate of the effect can be made by assuming a rectangular pulse with edge transition times $t_t = 2$ ns. The maximum 3 dB bandwidth of the pulse can be approximated by

$$f_w \cong \frac{0.35}{t_t} = 175 \; MHz \qquad (12)$$

The partial inductance contribution of the shunt, denoted by L_{1shunt}, was estimated by replacing the laser diode with a copper foil mounted flat on the PCB, and looking at the frequency of oscillation when switching Q_1 on. This yielded $L_{1shunt} = 1.21$ nH. Then the inductance was estimated with the shunt resistors mounted upside down, and finally it was measured with the shunt resistors replaced with copper foil. The results are shown in Table 2.

From Table 2, we can estimate that $L_{shunt,A} = 200$ pH for shunt resistors mounted right-side up and $L_{shunt,B} = 40$ pH for shunts mounted upside down, compared to no shunt. At $f_w = 175$ MHz, the inductive reactance for $L_{shunt,A}$ is

$$|Z_{shuntA}| = 2\pi f_w L_{shunt,A} = 0.176 \; \Omega \qquad (13)$$

The resistive value of the shunt should be at least 5x the inductive reactance, which would imply $R_{shunt,A} \geq 1.1$ Ω. This would result in a voltage drop of 39 V at the peak current, which is 40% of the transistor voltage rating. By mounting the shunt resistors upside down, we can reduce this by a factor of five to get $R_{shunt,B} \geq 0.22$ Ω. A final value of $R_{shunt} = 0.20$ Ω was chosen based on component availability.

Case	Test condition	Ringing frequency (MHz)	Estimated L_1 value (nH)
A	Shunts mounted normally	138	1.21
B	Shunts mounted upside down	148	1.05
C	Shunts replaced with foil	151	1.01

Table 2. Shunt inductance measurements

In order to see the effect of this on the waveform, Figure 14 shows the schematic for a simple simulation of a shunt with the three cases above, for $t_w = 3.3$ ns, and Figure 15 shows the results. It can be seen that even the small value of 200 pH (for 5 parallel 0402 resistors on the PCB) is enough to cause substantial error for short pulses. The effect of the inductance is to differentiate part of the current signal, exaggerating the initial part and peak of the waveform. The error becomes worse as the pulse gets shorter.

Unfortunately, it is difficult to mount resistors upside-down in a cost-effective manner, so boards as shipped that are represented by Case A. It may be possible to find a vendor willing to do this if there is a sufficient commercial incentive to do so. One manufacture already does this, but unfortunately the maximum value available is too small for good measurements at the time of writing [27]. If more accurate current measurements are desired, one may remount the resistors upside-down, use a larger value, or both. If the oscilloscope has a lowpass filter function with programmable frequency and a single-pole cutoff, one may attempt to cancel the zero in the response of the current shunt with a pole at the same frequency for more accurate results.

Dual edge control

As discussed, resonant capacitive discharge laser drivers have some useful properties. However, they do have a major limitation, namely that for a given power loop inductance, one has good control over the pulse height, but not the pulse width. Pulse width may also be used to control total pulse energy, and it can be easier to control than pulse amplitude, especially if such control is desired for individual pulses. Furthermore, in some cases, the laser diode or other load will need to be off the PCB. This necessitates some kind of interconnect which will add considerable inductance. In order to work with some of these limitations, one may use dual edge control, i.e. both turn-on and turn-off of the drive FET are used to control pulse shape.

In order to use the EPC9126xx with dual edge control, one must first recognize the limitations of the UCC27611 gate drive, which appears to have a minimum pulse width of approximately
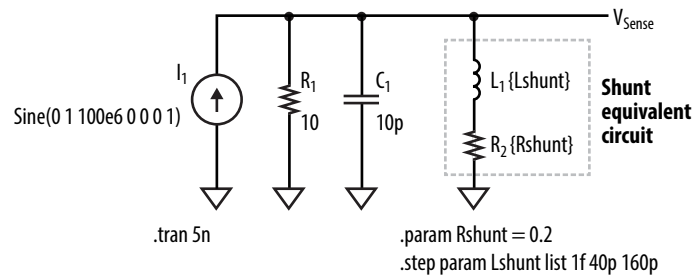

Figure 14. Simulation model of a typical shunt equivalent circuit.

6 ns, although this this not specified. This limits how short the pulse can be.

For typical dual edge control applications, the resonant capacitor and charging resistors will likely need to be changed. In the case where current must be limited, the charging resistor maybe used for this purpose, since there is additional bus capacitance at the bus voltage input to the PCB.

Finally, one must consider that the current in the power loop inductance will be interrupted when the switch is turned off, and this will cause ringing and overshoot on the drain terminal of the FET and the laser diode or other load. This ringing will depend on the inductance, the current at the time of turn-off, and the capacitance of the laser, FET, and PCB. There is a provision for the addition of some clamp diodes to control voltage overshoot.

Finding a suitable clamp diode is very challenging. Most diodes have package inductance on the same order as the power loop inductance, and this limits response speed. Furthermore, if the clamp current is high, the larger diode to handle this will tend to have

substantial capacitance that will contribute additional ringing, which in some cases can result in repeated undesired laser pulses. Unfortunately, the author cannot recommend a suitable clamp diode at this time.

When using the EPC9126xx for dual edge control applications, it is recommended that both careful simulation and experimentation is planned. The latter is especially important, as the author's experience is that for diodes selected to have the necessary voltage and current ratings, the available models do not accurately represent the behavior of the diodes for the extremely short transitions found in lidar applications.

Narrow pulse generator

A narrow pulse generator is also included on the EPC9126xx, based on the classic Jim Williams design [25]. By default, this circuit is not activated and the pulse input goes straight to the gate drive IC. However, by changing $0\ \Omega$ jumpers, one may make use of the circuit to generate very short pulses. The reader who desired to use this circuit should refer to Williams's application note.
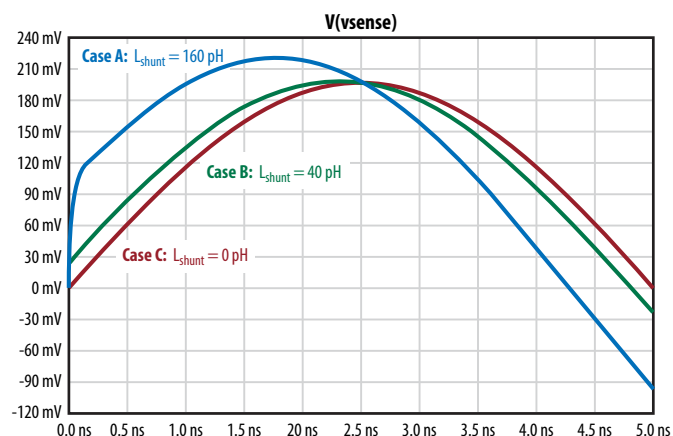

Figure 15. Results of simulation model from Figure 14 for three values of shunt series inductance.

Conclusions

The superior performance of GaN power transistors enable groundbreaking laser driver performance. The ability to generate single digit nanosecond, high current pulses to deliver hundreds of watts from a few square millimeters is truly remarkable. It is one of the main factors in making affordable, high performance lidar possible in a small form factor thus fueling the lidar revolution.

REFERENCES

[1] J. Glaser, "How GaN Power Transistors Drive High-Performance Lidar: Generating ultrafast pulsed power with GaN FETs," IEEE Power Electronics Magazine, vol. 4, Mar. 2017, pp. 25–35.

[2] P. McManamon, Field Guide to Lidar, SPIE, 2015.

[3] EPC9126 Lidar Demo Board (https://epc-co.com/epc/Products/DemoBoards/EPC9126.aspx)

[4] EPC9126HC Lidar Demo Board (https://epc-co.com/epc/Products/DemoBoards/EPC9126.aspx)

[5] OSRAM Opto Semiconductors Inc., "SPL PL90_3 Datasheet," 2015.

[6] Excelitas Technologies, "Surface Mount 905 nm Pulsed Semiconductor Lasers Datasheet," 2016.

[7] S. Morgott, "Range Finding Using Pulse Lasers," Regensberg, Germany: Osram Opto Semiconductors, 2004.

[8] S.A. Hovanessian, Radar System Design and Analysis, Norwood: Artech House, Inc, 1984.

[9] M. Andersson and J. Kjörnsberg, "Design of Lidar-system," Lund University, 2014.

[10] A. Lidow, J. Strydom, M. de Rooij, and D. Reusch, GaN Transistors for Efficient Power Conversion, Wiley, 2015.

[11] Efficient Power Conversion Corp., "EPC2016C data sheet," 2018.

[12] Efficient Power Conversion Corp., "EPC2022 data sheet," 2018.

[13] J. Glaser, " High Power Nanosecond Pulse Laser Driver using a GaN FET", PCIM Europe 2018 Proceedings, 2018.

[14] J.Glaser, " Kilowatt Laser Driver with 120 A, sub-10 nanosecond pulses in < 3 cm2 using a GaN FET", PCIM Asia 2018 Proceedings, 2018.

[15] R.W. Erickson and D. Maksimovic, Fundamentals of Power Electronics, Springer, 2001.

[16] M. Pavier, A. Woodworth, A. Sawle, R. Monteiro, C. Blake, and J. Chiu, "Understanding the Effect of Power MOSFET Package Parasitics on VRM Circuit Efficiency at Frequencies above 1 MHz," PCIM Europe 2003 Proceedings, 2003.

[17] D. Reusch, J. Strydom, and A. Lidow, "A new family of GaN transistors for highly efficient high frequency DC-DC converters," 2015 IEEE Applied Power Electronics Conference and Exposition (APEC), 2015, pp. 1979–1985.

[18] Velodyne Lidar Inc., "Velodyne Lidar Puck VLP-16 data sheet," 2017.

[19] D. Reusch and J. Strydom, "Understanding the effect of PCB layout on circuit performance in a high frequency gallium nitride based point of load converter," 2013 Twenty-Eighth Annual IEEE Applied Power Electronics Conference and Exposition (APEC), 2013, pp. 649–655.

[20] Efficient Power Conversion Corp., "EPC9126 Lidar Development Board Quick Start Guide, Rev. 2.5," 2016.

[21] Efficient Power Conversion Corp., "EPC9126HC Lidar Development Board Quick Start Guide, Rev. 1.0," 2017.

[22] H. Johnson and M. Graham, High-Speed Digital Design – A Handbook of Black Magic, Prentice Hall PTR, 1993.

[23] J. Weber, Oscilloscope Probe Circuits, Tektronix Inc., 1969.

[24] Tektronix Inc, "20X Low Capacitance Probe – P6158 Datasheet," 2017, (https://download.tek.com/datasheet/P6158-Datasheet-60W120263_0.pdf)

[25] J. Williams, "AN98 Signal Sources, Conditioners, and Power Circuitry – Circuits of the Fall, 2004: Nanosecond Pulse Width Generator," Linear Technology Corporation, 2004.

[26] http://ucanr.edu/blogs/green//blogfiles/11605_original.png

[27] Susumu 2018 Product Catalogue (EN), 2018-04-06, pp. 53-54. 2018, (https://www.susumu.co.jp/common/pdf/n_catalog_partition09_en.pdf?v=20180406)